

Heat Transfer of Mixed Convection Electroconductivity Flow of Copper Nanofluid with Different Shapes in a Porous Micro Channel Provoked by Radiation and First Order Chemical Reaction

Abstract:

This work presents a theoretical description of different shapes of copper nanoparticle in water based fluid. Analytical solution of the governing hydrodynamic equations and graphs plotted using Mathematica 9.0 software, showed that heat transfer is rapid due to the presence of radiation. Increase in radiation and chemical reaction also led to a corresponding increase in the temperature and concentration profiles of the nanofluid respectively. For the velocity profile of the nanofluid, nanoparticles volume fraction is the only parameter that its increase, increases the velocity profile of the copper nanofluid but Reynolds number, Grashof's number and electroconductivity, result to decrease in the velocity profile of the copper nanofluid. The effect of Nusselt number, Sherwood number and skin friction on the nanofluid is also determined.

Key Words- : Heat transfer, Copper, Nanofluid, Porous Channel, Water Based Fluid

Notation

ρ_{nf}	density of nanofluid
P	pressure of fluid
u	dimensionless fluid velocity
μ_{nf}	dynamic viscosity of nanofluid
$(\rho\beta)_{nf}$	thermal expansion coefficient of nanofluids due to temperature
σ_{∞}	constant fluid electronconductivity
U	plate velocity
k_0	porosity of the medium
k_{nf}	thermal conductivity of nanofluid
q	radiative heat flux
g	acceleration due to gravity
k_f	thermal conductivity of base fluid
ϕ	nanoparticles volume fraction
ρ_f	density of base fluid

40	ρ_s	density of nanoparticles
41	$(\rho C_p)_{nf}$	heat capacitance of nanofluids
42	β_s	volumetric coefficient of nanoparticles
43	β_f	volumetric coefficient of base fluid
44	$(C_p)_f$	specific heat capacity of base fluid
45	$(C_p)_s$	specific heat capacity of nanoparticles
46	C'	concentration of fluid
47	C	dimensionless concentration of fluid
48	T	temperature of fluid
49	θ	dimensionless temperature of fluid
50	Re	Reynolds number
51	Pe	Peclet number
52	Gr_T	thermal Grashof number
53	Gr_C	concentration Grashof number
54	N	dimensionless radiation term
55	k_∞	dimensionless chemical reaction term
56	k_r^2	chemical reaction term
57	λ_n	thermal conductivity ratio
58	D_{nf}	molecular diffusivity
59	u'	fluid velocity

1. Introduction

Thermal conductivity of heat transfer in fluids is key in the development of energy efficient heat transfer equipment. Conventional heat transfer fluids such as water, oil, ethylene glycol mixtures to mention few, are poor heat transfer fluids. With global need for improvement, to develop advanced heat transfer fluids with significantly higher thermal conductivities than those presently available is of utmost necessity. Touloukian et al (1970) has opined that at room temperature, metals in solid form have orders of magnitude higher that those of solids. The new class of heat transfer fluids that are engineered by suspending nanometer-sized particles in conventional heat transfer fluids whose averaged sized particles is below 50nm is termed nanofluids Choi (1995) The reality is that in today's science and technology, size does matter, therefore modern fabrication technology provides great opportunity to actively process materials at the micro and nanometer scales. The impact of this new heat transfer technology is important due to its performance in thermal conductivity and viscosity which led to improved heat transfer and stability, reduced pumping power, minimal clogging and miniaturized systems as well as cost and energy savings (Choi et al 1992a and 1992b). The different composition of nanoparticles in base fluids to form nanofluids has its application in power generation and electronic equipment just to mention few. The applications of nanofluids is predicated on the desirable properties or qualities following Mukherjee and Paria (2013) as follows (i) rapid

increase in thermal conductivity (ii) ultrafast heat transfer ability (iii) reduce pumping power (iv) reduce friction coefficient (v) reduce clogging in microchannels (vi) improved stability than other colloids and (vii) improved lubrication. Feng et al (2006), examined the preparation of gold, silver and platinum nanofluids using aqueous organic phase transfer method. Yu et al (2010) Wei et al (2010) and Zhu et al (2007), prepared Copper oxide nanofluid and use ammonium citrate to prevent the growth and aggregation of nanoparticles, resulting in a stable CuO aqueous nanofluid with higher thermal conductivity. Other works such as (Hwang, et al (2007) and Li et al(2007), used spectral analysis method to detect stability of nanofluids. Experimental and theoretical studies are abound on conductivity, viscosity and stability of nanofluids and its aggregate nanoparticles. Duncan and Rouvray (1989), Glaser(1989) and Hashin and Shtrikman (1962) examined nanofluid materials and made far reaching deductions from their findings. The model proposed by Hamilton and Crosser (1962) to predict the thermal conductivity of nanofluid, containing large agglomerated particles and that obtained from experimental results were compared and it fits well, but divergence is observed at low volume fractions. The implication of this observation is that particle size and shape dominate thermal conductivity of nanofluids (Li 1998). Studies on nanoparticles of spherical shapes are many but limited in applications and significance, Aaiza et al (2015). As a result of this assertion, a non spherical shaped nanoparticle is chosen for this study in four different shapes, namely, platelet, cylinder, blade and brick. The choice of non spherical shape nanoparticle is predicated on the work of Aaiza et al (2015), where they mentioned desirable properties in cancer treatment. Asma et al (2015), studied free convection flow of nanoparticles including ramped wall temperature using five different types of spherical shape nanoparticles and reported that the solution of the governing equations was exact. Heat transfer due to mixed convection is experienced in many physical situations and occur as the flow in a channel due to the process of heating or cooling of the channel walls. This experience is a combination of free convection and forced convection. Some researches have been reported, they include (Sebdani et al (2012), Sheikhezabeh et al (2012), Nadeem and Saleem (2014) and Al-Salem et al(2012) in which mixed convection and nanofluid were discussed in different nanoparticles shape and configurations. Aaiza et al (2015), investigated water based nanofluid and ethylene glycol based nanofluid and reported that viscosity and thermal conductivity are the most prominent parameters responsible for different results of velocity and temperature. The present study is to examine the effect of first order chemical reaction and electroconductivity on radiative heat transfer in mixed convection flow in a micro porous channel with different shapes of copper (Cu) in water based nanofluid. The Cu in water based nanofluid preparation and sphericity is reported in Yimin and Li (2000). The reason is that Cu as a nanoparticle, possesses higher thermal conductivity and stability than other nanofluids. The focus is to consider non spherical shaped nanofluid under the no slip boundary conditions with bounding walls of the channel at rest, the upper wall in motion and lower at rest and both walls are in motion. Solutions to velocity, temperature and concentration profile with graphical results and

parameters of interest discussed, which is an extension of the work of Aaiza et al (2105)

2. Formulation of the problem

The assumption of the effect of induced magnetic field is small, therefore, neglected. Also the usual Boussinesq approximation is assumed. The no slip condition at the boundary wall is considered. The x-axis is taken along the flow and y-axis is taken normal to the flow direction. The governing hydrodynamic equations are given as

$$\rho_{nf} \frac{\partial u'}{\partial t'} = -\frac{\partial p}{\partial x'} + \mu_{nf} \frac{\partial^2 u'}{\partial y'^2} - u' \left(\frac{\sigma_\infty}{U} + \frac{\mu_{nf}}{k_0} \right) + (\rho\beta_T)_{nf} g(T - T_0) + (\rho\beta_c)_{nf} g(C - C_0) \quad (1)$$

$$(\rho C_p)_{nf} \frac{\partial T}{\partial t'} = k_{nf} \frac{\partial^2 T}{\partial y'^2} - \frac{\partial q}{\partial y} \quad (2)$$

$$(\rho C_p)_{nf} \frac{\partial C'}{\partial t'} = D_{nf} \frac{\partial^2 C'}{\partial y'^2} - k_r^2 C' \quad (3)$$

With the boundary conditions

$$u'(0, t) = 0, \quad u'(d, t) = 0, \quad (4)$$

$$T(0, t) = T_0, \quad T(d, t) = T_w \quad (5)$$

$$C'(0, t) = C_0, \quad C'(d, t) = C_w \quad (6)$$

where following Boricic et al. (2005), the fluid electroconductivity is assumed to be of

the form $\sigma_\infty \left(1 - \frac{u'}{U} \right)$ but for physical exigency and mathematical amenability, it is

approximated to the form in equation (1) Ngiangia and Harry (2017).

According to a model proposed by Hamilton and Crosser (1962), the thermal conductivity and dynamic viscosity is assumed valid for both spherical and non spherical shapes nanoparticles. The model is stated as

$$\mu_{nf} = \mu_f (1 + a\phi + b\phi^2) \quad (7)$$

$$\frac{k_{nf}}{k_f} = \frac{k_s + (n-1)k_f + (n-1)(k_s - k_f)\phi}{k_s + (n-1)k_f - (k_s - k_f)\phi} \quad (8)$$

where $n = \frac{3}{\psi}$ is the empirical shape factor and ψ is the sphericity, a ratio of surface area of sphere to surface area of real particle with equal volumes as in **table 1** with **a** and **b** as constant empirical shape factors.

Another expression by Wasp(1977) to determine the effective thermal conductivity of solid-liquid mixture is given as

$$\frac{k_{eff}}{k_f} = \frac{k_s + 2k_f - 2\phi(k_f - k_s)}{k_s + 2k_f - \phi(k_f - k_s)} \quad (9)$$

This is a special case of equation (8) with sphericity 1.0

From equations (1), (2) and (3), ρ_{nf} , $(\rho\beta)_{nf}$ and $(\rho C_p)_{nf}$ following Asma et al (2015) is derived as

$$\begin{aligned} \rho_{nf} &= (1-\phi)\rho_f + \phi\rho_s \\ (\rho\beta)_{nf} &= (1-\phi)(\rho\beta)_f + \phi(\rho\beta)_s \\ (\rho C_p)_{nf} &= (1-\phi)(\rho C_p)_f + \phi(\rho C_p)_s \end{aligned} \quad (10)$$

In the work of Makinde and Mhone (2005), the plates temperature T_0 and T_w are usually high and produces radiative heat transfer. According to Cogley et al (1968), for optically thin medium with relatively low density, the radiative heat flux is given by

$$\frac{\partial q}{\partial y} = 4\delta^2(T - T_0) \quad (11)$$

where δ is the radiation absorption coefficient

Substituting equation (11) into equation (2) and using the following dimensionless variables

$$\begin{aligned} x &= \frac{x'}{d}, y = \frac{y'}{d}, u = \frac{u'}{U}, t = \frac{t'U}{d}, \frac{\partial p}{\partial x'} = \lambda \exp(i\omega t), \theta = \frac{T - T_0}{T_w - T_0}, \text{Re} = \frac{Ud}{\mu_f} \\ k &= \frac{k_0}{d^2}, Gr_T = \frac{g\beta_f d^2 (T_w - T_0)}{\mu_f U}, Gc_T = \frac{g\beta_c d^2 (C' - C_0)}{\mu_f U}, \sigma_0 = \frac{\sigma_\infty \mu_f dt}{U} \\ N &= \frac{4\delta^2 d^2}{k_f}, Pe_T = \frac{Ud(\rho C_p)_f}{k_f}, Pe_c = \frac{Ud(\rho C_p)_f}{D_{nf}}, k_\infty = \frac{k_r^2 T_0}{\sigma_\infty U^2}, \lambda_n = \frac{k_{nf}}{k_f} \end{aligned}$$

Further, we define

$$w_1 = (1-\phi) + \phi \frac{\rho_s}{\rho_f} \quad w_2 = (1 + a\phi + b\phi^2) \quad w_3 = (1-\phi)\rho_f + \phi \frac{(\rho\beta)_s}{\beta_f}$$

$$w_4 = \left[(1-\phi) + \phi \frac{(\rho C_p)_s}{(\rho C_p)_f} \right] \quad a_1 = w_1 \text{Re} \quad a_2 = \sigma_0 + \frac{w_2}{k} \quad a_3 = w_3 Gr_T$$

$$a_4 = w_3 Gr_c, c_1 = \frac{Pe_c w_4}{\lambda_n} \quad b_1 = \frac{Pe_T w_4}{\lambda_n} \quad b_2 = \frac{N}{\lambda_n}, c_2 = \frac{k_\infty}{\lambda_n},$$

then equations (1), (2) and (3) takes the form

$$a_1 \frac{\partial u}{\partial t} = \lambda \varepsilon \exp(i\omega t) + w_2 \frac{\partial^2 u}{\partial y^2} - a_2 u + a_3 \theta + a_4 C \quad (12)$$

$$b_1 \frac{\partial \theta}{\partial t} = \frac{\partial^2 \theta}{\partial y^2} - b_2 \theta \quad (13)$$

$$c_1 \frac{\partial C}{\partial t} = \frac{\partial^2 C}{\partial y^2} - c_2 C \quad (14)$$

Subject to the boundary conditions

$$u(0, t) = 0, \quad u(1, t) = 1 \quad t > 0 \quad (15)$$

$$\theta(0, t) = 0, \quad \theta(1, t) = 1 \quad t > 0 \quad (16)$$

$$C(0, t) = 0, \quad C(1, t) = 1 \quad t > 0 \quad (17)$$

195

196 3. Method of Solution

197

198 To solve equations (12-14), we assume solution of the form

199

$$u(y, t) = [u_0(y) + \varepsilon \exp(i\omega t)u_1(y)] \quad (18)$$

$$\theta(y, t) = [\theta_0(y) + \varepsilon \exp(i\omega t)\theta_1(y)] \quad (19)$$

$$C(y, t) = [C_0(y) + \varepsilon \exp(i\omega t)C_1(y)] \quad (20)$$

203 where ε is a small parameter

204

205 **Case 1:** Both walls of the channel are kept stationary, while the temperature of the upper
206 wall of the channel is assumed constant, the lower wall has uniform temperature and the
207 boundary conditions conform to equations (18-20).

208 We substitute equation (20) into equation (14) and simplify, the result is

209

$$C_0''(y) - c_2 C_0(y) = 0 \quad (21)$$

$$C_1''(y) - (c_1 i\omega + c_2)C_1(y) = 0 \quad (22)$$

212 Solving equations (21) and (22) and imposing the boundary conditions of equation (17)
213 as well as substituting in equation (20), we get

$$C(y, t) = \sinh\sqrt{c_2} y + \varepsilon \exp(i\omega t) \sinh\sqrt{\beta} y \quad (23)$$

215 where $\beta = c_1 i\omega + c_2$

216 Similarly, we put equation (19) into equation (13) and the resulting expression takes the
217 form

218

$$\theta_0''(y) - b_2 \theta_0(y) = 0 \quad (24)$$

$$\theta_1''(y) - (b_1 i\omega + b_2)\theta_1(y) = 0 \quad (25)$$

221 The solutions of equations (24) and (25) and imposition of the boundary conditions of
222 equation (16) as well as put the entire expression into equation (19), gives

223

$$\theta(y, t) = \sinh\sqrt{b_2} y + \varepsilon \exp(i\omega t) \sinh\sqrt{\beta_2} y \quad (26)$$

225 where $\beta_2 = b_1 i\omega + b_2$

Also, following the same procedure and the boundary conditions of equation (18), the solution of equation (12) is

$$u(y,t) = \beta_5 \sinh \sqrt{\frac{a_2}{w_2}} y + \beta_3 \sinh \sqrt{b_2} y + \beta_4 \sinh \sqrt{c_2} y + \varepsilon \exp(i\omega t) \left(-\beta_8 \cosh \sqrt{\frac{a_1 + a_2}{w_2}} y + \beta_9 \sinh \sqrt{\frac{a_1 + a_2}{w_2}} y + \beta_6 \sinh \sqrt{\beta_2} y + \beta_7 \sinh \sqrt{\beta} y + \beta_8 \right) \quad (27)$$

$$\text{where, } \beta_3 = \frac{-\frac{a_3}{w_2}}{b_2^2 - \frac{a_2}{w_2}}, \quad \beta_4 = \frac{a_4}{w_2(c_2^2 - 1)}, \quad \beta_5 = \frac{-\beta_3 \sinh \sqrt{b_2} - \beta_4 \sinh \sqrt{c_2}}{\sinh \sqrt{\frac{a_2}{w_2}}},$$

$$\beta_6 = \frac{-\frac{a_3}{w_2}}{\beta_2 - \frac{a_1 + a_2}{w_2}}, \quad \beta_7 = \frac{-\frac{a_4}{w_2}}{\beta - \frac{a_1 + a_2}{w_2}}, \quad \beta_8 = \frac{\lambda}{a_1 + a_2},$$

$$\beta_9 = \frac{-(\beta_8 + \beta_6 \sinh \sqrt{\beta_2} + \beta_7 \sinh \sqrt{\beta})}{\sinh \sqrt{\frac{a_1 + a_2}{w_2}}}$$

Case 2: The upper wall of the channel is set into oscillatory motion while the lower wall is held stationary and the resulting boundary conditions are given as

$$u(0,t) = 0, \text{ and } u(1,t) = H(t)\varepsilon \exp(i\omega t); \quad t > 0 \quad (28)$$

where $H(t)$ is the Heaviside step function

Imposing the boundary conditions of equation (28) into the solution of equation (12), we get

$$u(y,t) = \left(\frac{H(t)\varepsilon \exp(i\omega t) - \beta_3 \sinh \sqrt{b_2} - \beta_4 \sinh \sqrt{c_2}}{\sinh \sqrt{\frac{a_2}{w_2}}} \right) \sinh \sqrt{\frac{a_2}{w_2}} y + \beta_3 \sinh \sqrt{b_2} y + \beta_4 \sinh \sqrt{c_2} y + \varepsilon \exp(i\omega t) \left[\left(\frac{H(t)\varepsilon \exp(i\omega t) - \beta_6 \sinh \sqrt{\beta_2} - \beta_7 \sinh \sqrt{\beta} - \beta_8}{\sinh \sqrt{\frac{a_1 + a_2}{w_2}}} \right) \sinh \sqrt{\frac{a_1 + a_2}{w_2}} y + \beta_{10} \right] \quad (29)$$

where $\beta_{10} = \beta_6 \sinh \sqrt{\beta_2} y + \beta_7 \sinh \sqrt{\beta} y + \beta_8$

Case 3: In this situation, the two channel walls are set into oscillatory motion and the resulting boundary conditions (Aiza et al (2105)) are given as

$$u(0, t) = H(t) \varepsilon \exp(i\omega t) \text{ and } u(1, t) = H(t) \varepsilon \exp(i\omega t) \quad t > 0 \quad (30)$$

The solution of equation (12), having used the boundary conditions of equation (30), following the same procedure used in case 2, we obtain

$$\begin{aligned} u(y, t) = & H(t) \varepsilon \exp(i\omega t) \cosh \sqrt{\frac{a_2}{w_2}} y + \\ & \left(\frac{H(t) \varepsilon \exp(i\omega t) - \beta_3 \sinh \sqrt{b_2} - \beta_4 \sinh \sqrt{c_2}}{\sinh \sqrt{\frac{a_2}{w_2}}} \right) \sinh \sqrt{\frac{a_2}{w_2}} y \\ & + \beta_3 \sinh \sqrt{b_2} y + \beta_4 \sinh \sqrt{c_2} y \\ & + H(t) \varepsilon \exp(i\omega t) \cosh \sqrt{\frac{a_1 + a_2}{w_2}} y + \\ & \left(\frac{H(t) \varepsilon \exp(i\omega t) - \beta_6 \sinh \sqrt{\beta_2} - \beta_7 \sinh \sqrt{\beta} - \beta_8}{\sinh \sqrt{\frac{a_1 + a_2}{w_2}}} \right) \sinh \sqrt{\frac{a_1 + a_2}{w_2}} y \\ & + \beta_6 \sinh \sqrt{\beta_2} y + \beta_7 \sinh \sqrt{\beta} y + \beta_8 \end{aligned} \quad (31)$$

Nusselt number (Nu) (the rate of heat transfer coefficient)

From equation (26), the Nusselt number is given by

$$Nu = - \left(\frac{\partial \theta}{\partial y} \right)_{y=0} = - \left(\sqrt{b_2} + \varepsilon \exp(i\omega t) \sqrt{\beta_2} \right) \quad (32)$$

Sherwood number (S_b) (the rate of mass transfer coefficient)

$$S_b = - \left(\frac{\partial C}{\partial y} \right)_{y=0} = - \left(\sqrt{C_2} + \varepsilon \exp(i\omega t) \sqrt{\beta} \right) \quad (33)$$

Skin frictions (τ)

$$\left(\frac{\partial u}{\partial y} \right)_{y=0} = \beta_5 \sqrt{\frac{a_2}{w_2}} + \beta_3 \sqrt{b_2} + \beta_4 \sqrt{c_2} + \varepsilon \exp(i\omega t) \left(\beta_9 \sqrt{\frac{a_1 + a_2}{w_2}} + \beta_6 \sqrt{\beta_2} + \beta_7 \sqrt{\beta} \right) \quad (34)$$

Case 2

$$\left(\frac{\partial u}{\partial y}\right)_{y=0} = \left[\frac{H(t)\varepsilon \exp(i\omega t) - \beta_3 \sinh\sqrt{b_2} - \beta_4 \sinh\sqrt{c_2}}{\sinh\sqrt{\frac{a_2}{w_2}}} \right] \sqrt{\frac{a_2}{w_2}} + \beta_3\sqrt{b_2} + \beta_4\sqrt{c_2} + \varepsilon \exp(i\omega t) \left[\frac{H(t)\varepsilon \exp(i\omega t) - \beta_6 \sinh\sqrt{\beta_2} - \beta_7 \sinh\sqrt{\beta} - \beta_8}{\sinh\sqrt{\frac{a_1 + a_2}{w_2}}} \right] \sqrt{\frac{a_1 + a_2}{w_2}} + \beta_{77} \right] \quad (35)$$

where $\beta_{77} = \beta_6\sqrt{\beta_2} + \beta_7\sinh\sqrt{\beta}$

Case 3

$$\left(\frac{\partial u}{\partial y}\right)_{y=0} = \left[\frac{H(t)\varepsilon \exp(i\omega t) - \beta_3 \sinh\sqrt{b_2} - \beta_4 \sinh\sqrt{c_2}}{\sinh\sqrt{\frac{a_2}{w_2}}} \right] \sqrt{\frac{a_2}{w_2}} + \beta_3\sqrt{b_2} + \beta_4\sqrt{c_2} + \left[\frac{H(t)\varepsilon \exp(i\omega t) - \beta_6 \sinh\sqrt{\beta_2} - \beta_7 \sinh\sqrt{\beta} - \beta_8}{\sinh\sqrt{\frac{a_1 + a_2}{w_2}}} \right] \sqrt{\frac{a_1 + a_2}{w_2}} + \beta_6\sqrt{\beta_2} + \beta_7\sqrt{\beta} \right] \quad (36)$$

4. Discussion

As a result of increase in the chemical reaction of the nanoparticles and the base fluid, a corresponding increase in the concentration of the nanofluid is observed as depicted in Figure 1

Figure 2, showed the effect of radiation on the temperature of copper nanofluid. As a result of high thermal conductivity of nanofluid, increase in radiation of nanofluid result in a corresponding increase in the temperature profile of the nanofluid. This observation is consistent with the work of Aaiza et al (2015) and Timofeeva et al (2009) and a departure from the effect of radiation on other base fluids.

Figure 3, showed the convective heat transfer coefficient between the nanofluid and the channel walls to estimate the heat transfer performance of the nanofluid. The graph showed that, the heat transfer is rapid (a curve), may be due to the presence of radiation when compared to the work of Xuan and Li (2000) which is a straight line. The peclet number is a parameter to describe such effect. Equation (32) therefore, is a holistic approach to study the improved heat transfer mechanism of the nanofluid.

From Figure 4, it is shown that the relationship can be used to determine the convective mass transfer coefficient between the nanofluid and the containing inner wall to estimate the improved mass transfer performance of the nanoparticles.

Figure 5, clearly demonstrate that, increase in peclet number correspond to a decrease in the skin friction of the nanofluid.

Increase in nanoparticles volume fraction of copper nanofluid result in a corresponding increase in the velocity profile of the nanofluid as shown in Figure 6.

Reynolds number describe the transition of fluids from laminar to turbulence, since it is a ratio of inertia force to viscous force, its increase as shown in Figure 7, results in a decrease in the velocity profile of nanofluid and this observation is at variance with the results of increase in Reynolds number of base fluids(Ngiangia and Taylor-Harry 2017). Electroconductivity tends to impede the flow of fluid and same observation was noticed as depicted in Figure 8, where increase in electroconductivity enhances the decrease in the velocity of copper nanofluid.

The Grashof number due to temperature conducts heat away from the channel plates into the nanofluid, thereby increasing the temperature of the fluid but as a result of rapid heat transfer and thermal conductivity of nanofluid, a decrease in velocity profile of the nanofluid is observed as shown in Figure 9.

Figure 10, showed the effect of different shapes of copper nanoparticles on the velocity of water based nanofluids. The graph clearly depicts that, the highest velocity is recorded with brick followed by cylinder, platelet and finally blade. The effect on shapes of nanoparticles on velocity is also a dependence on viscosity for various volume fractions.

The following numerical values are used in the plotting of the graphs

$$\lambda_n = 100, \omega = 0.2, t = 1, \lambda = 1, \varepsilon = 0.003, k = 0.3$$

$$Gr_T, Gr_C = 1, 3, 5, 7$$

$$Pe = 0.35, 0.70, 1.05, 1.40$$

$$\phi = 0.1, 0.2, 0.3, 0.4$$

$$Re = 100, 1500, 2000, 2500$$

$$N = 2.0, 4.0, 6.0, 8.0$$

$$k_\infty = 1.35, 2.35, 3.35, 4.45$$

$$\sigma_0 = 0.4, 0.8, 1.2, 1.6$$

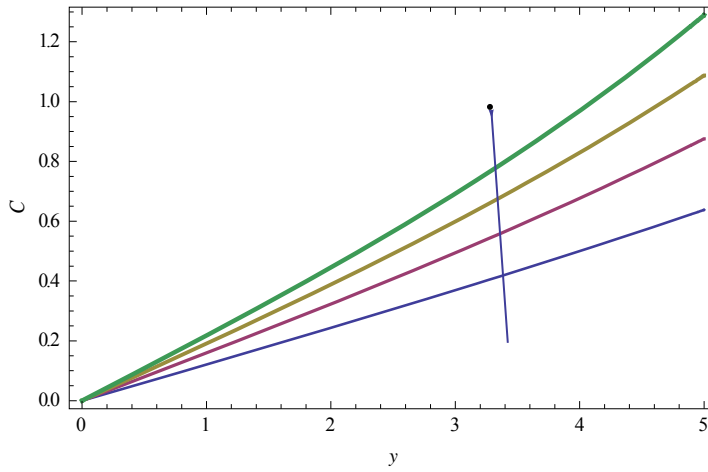


Fig.1. The dependence of concentration on coordinate with chemical reaction k_{∞} varying

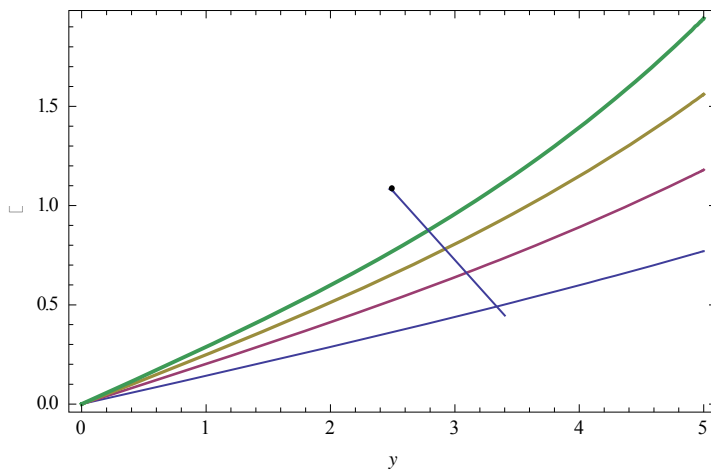


Fig.2. The dependence of temperature on coordinate with radiation N varying

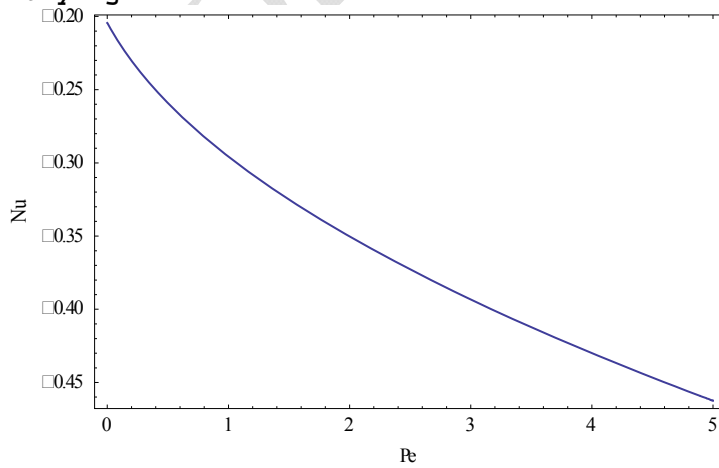


Fig.3. The Nusselt number(Nu) versus Peclet number(Pe)

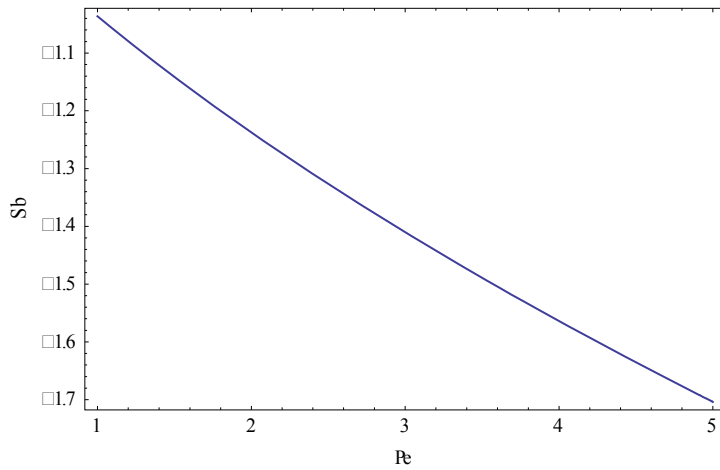


Fig.4. The Sherwood number (S_b) versus Peclet number (Pe)

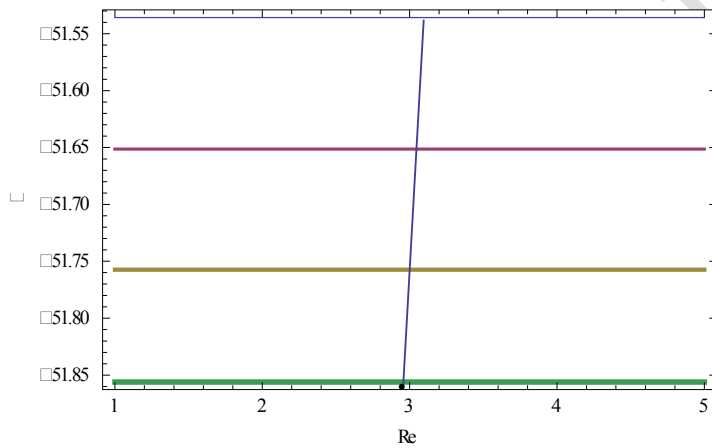


Fig.5. The Skin Friction (τ) versus Reynolds number (Re) with Peclet number (Pe) varying.

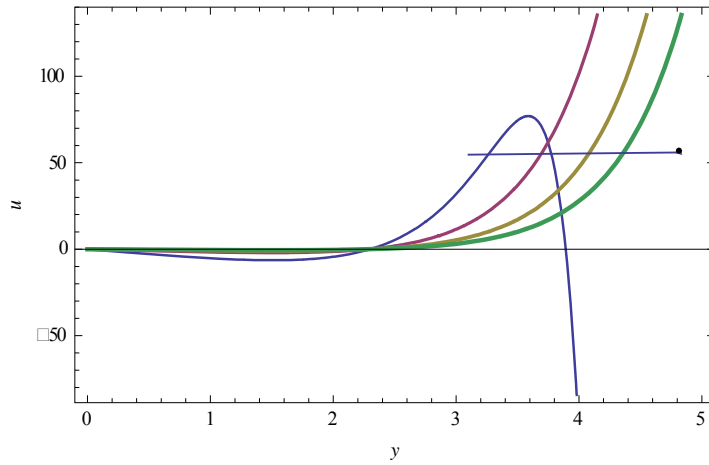


Fig.6. The dependence of velocity on coordinate with nanoparticles volume fractions ϕ varying

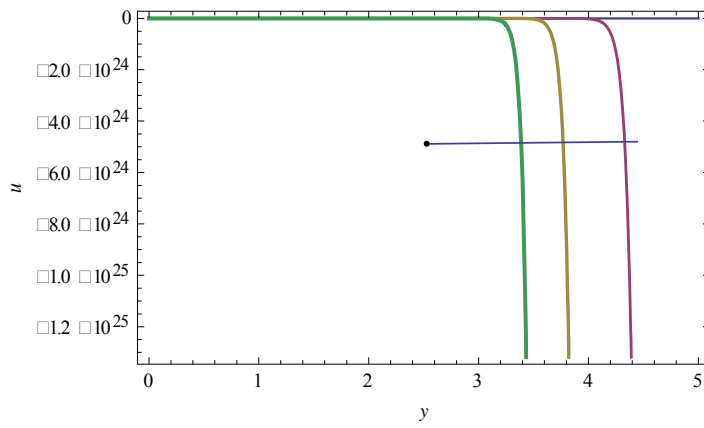


Fig.7. The dependence of velocity on coordinate with Reynolds number Re varying

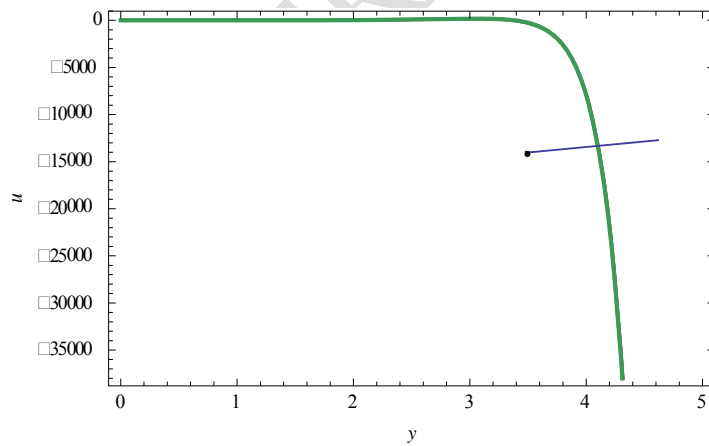


Fig.8. The dependence of velocity on coordinate with conductivity σ_0 varying

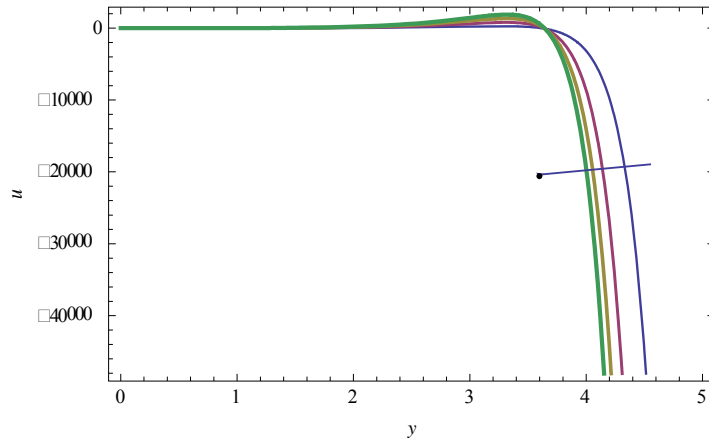


Fig.9. The dependence of velocity on coordinate with Grashof number Gr_T varying

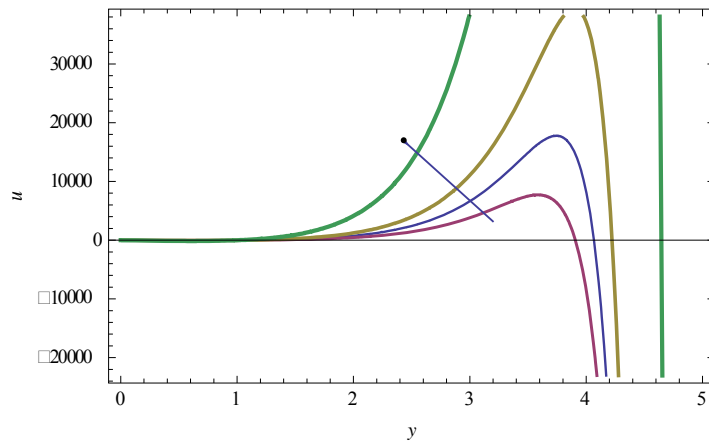


Fig.10. The dependence of velocity on coordinate with different nanoshape particles n

Table 1: Constants **a** and **b** empirical shape factors, Timofeeva et al (2009)

Model	Platelet	Blade	Cylinder	Brick
a	37.1	14.6	13.5	1.9
b	612.6	123.3	904.4	471.4

Table 2: Sphericity for different shapes nanoparticles, Timofeeva et al (2009)

Model	Platelet	Blade	Cylinder	Brick
ψ	0.52	0.36	0.62	0.81

Table 3: Thermophysical properties of water and nanoparticle, Timofeeva et al (2009)

Model	$\rho(kgm^{-3})$	$C_p(kg^{-1}K^{-1})$	$k(Wm^{-1}K^{-1})$	$\beta \times 10^{-5} K^{-1}$
Water(H_2O)	997.1	4179	0.613	21
Copper(Cu)	8933	385	401	1.67

5. Conclusions

A perturbation technique on the description of the heat and mass transfer of copper nanofluid has been carried out. An essential characteristic of nanofluid, in particular copper nanoparticles in water based fluids is that, as a result of its high thermal conductivity and heat transfer ability, the effect on velocity profile is significantly different from other conventional base fluids. Experiments is needed for industrial, scientific and engineering applications of copper nanaofluid and others. It should be noted that the improved performance of the copper nanofluid is not limited to its high thermal conductivity and heat transfer ability but also from the random movement and dispersion effect on the nanoparticles. The effect of Grashof number on the concentration of nanofluid was ignored because the result is the same as that of the temperature.

REFERENCES

- Aaiza, G; Khan I and Shafie S. 2015. Energy Transfer in Mixed Convection MHD Flow of Nanofluid Containing Different Shapes of Nanoparticles in a Channel Filled with Saturated Porous Medium. *Nanoscale Research Letters*. 10(490): 1-14.
- Al-Salem, K, Oztop, H. F, Pop, I and Varo, Y. 2012. Effect of Moving lid Direction on MHD Mixed Convection in a linearly Heated Cavity. *International Journal of Heat and Mass Transfer*. 55, 1103-1112.
- Asma, K, Khan, I and Sharidan, S 2015. Exact Solutions for Free Convection Flow of NanoFluids with Ramped Wall Temperature. *The European Physical Journal Plus*. 130, 57-71.
- Boricic, Z, Nikodijevic D, Milenkovic D, and Stamenkovic Z. 2005. A form of MHD universal equation of unsteady incompressible fluid flow with variable electroconductivity on heated moving plate *Theoretical and Applied Mechanics*. 32(1), 65-77.
- Choi, U. S,. 1995. Enhancing Thermal Conductivity of Fluids with Nanoparticles. *Development and Applications of Non-Newtonian Flows*. Eds. D. A. 99-105.
- Choi, U. S, Cho, Y. I and Kasza, K. E. 1992a. Degradation effects of dilute Polymer Solutions on Turbulent Friction and Heat Transfer Behaviour. *Journal of Non-Newtonian Fluid Mechanics*. 41, 289-307
- Choi, U. S, France, D. M and Knodel, B. D. 1992b. Impact of advanced Fluids on Costs of districts Cooling Systems. *Proceedings of 83rd Annual International Districts Heating and Cooing Association Confrence*. Danves, Washington D C. 343-359.
- Cogley, A. C, Vincent, W. G, Giles, S. E. 1968. Differential approximation to radiative heat transfer in a non-grey gas near equilibrium, *The American Inst. Aeronautics and Astronautics*. 6:551-553.
- Duncan, M. A and Rouvray, D. H, 1989. Microclusters. *Scientific American*, 110-115.

- Feng, X, Ma, H and Huang S. 2006. Aqueous-organic phase-transfer of highly stable gold, silver, and platinum nanoparticles and new route for fabrication of gold nanofilms at the oil/water interface and on solid supports, *Journal of Physical Chemistry B*. 110(25) 12311–12317.
- Gleiter, H, (1989). *Nanocrystalline Materials*. Programme on Materials Science. 33, 223-315.
- Hamilton, R. L and Crosser, O. K, 1962. Thermal Conductivity of Heterogeneous Two-Component Systems. *Journal of Industrial and Engineering Chemistry Fundamentals*. 1(3), 187-191.
- Hashin, Z and Shtrikman, S 1962. A variational Approach to the Theory of the Effective Magnetic Permeability of Multiphase Materials. *Journal of Applied Physics*. 33(10), 3125-3131.
- Hwang, Y, Lee, J. K. Lee, C. H . 2007. Stability and thermal conductivity characteristics of nanofluids, *Thermochimica Acta*, 455(1-2),70–74.
- Li, B. C .,1998. Nanotechnology in China. *Journal of Aerosol Science*. 29(5/6), 751-755.
- Li, X. Zhu, D. and Wang, X. 2007. Evaluation on dispersion behavior of the aqueous copper nanosuspensions, *Journal of Colloid and Interface Science*. 310(2) 456–463.
- Makinde, O. D and Mhone, P. Y. 2005. Heat Transfer to MHD Oscillatory Flow in a Channel Filled with Porous Medium. *Romanian Journal of Physics*. 50, 931-938.
- Mukherjee, S and Paria, S. 2013. Preparation and Stability of Nanofluids-A Review. *IOSR Journal of Mechanical and Civil Engineering*. 9(2), 63-69
- Nadeem, S and Saleem, S. 2004. Unsteady Mixed Convection Flow of Nanofluid on a rotating cone with Magnetic Field. *Apply Nanoscience*. 4, 405-414.
- Ngangia, A.T and Harry, S T. 2017. Electroconductivity of Steady Viscous MHD Incompressible Fluid Between Two Porous Parallel Plates Provoked by Chemical Reaction and Radiation. *Physical Science International Journal* 13(2): 1-13.
- Sebdani, S, Mahmoodi, M and Hashemi, S 2012. Effect of Nanofluid Variable Properties on mixed Convection in a Square Cavity. *International Journal of Thermodynamic Science*. 52, 112-126.
- Sheikhezabeh, G. A, Hajialigol, N, Qomi, M. E and Fattahi, A. 2012. laminar Mixed Convection of Cu-water Nanofluid in two sided lid-driven Enclosures. *Journal of Nanostuctures*. 1, 44-53
- Wasp, F., 1977. *Solid-Liquid Flow Slurry Pipeline Transportation*. Trans. Tech. Pub., Berlin.

Wei, X and Wang, L. 2010. Synthesis and thermal conductivity of microfluidic copper nanofluids, *Particuology*. 8(3), 262– 271.

Xuan, Y and Li, Q., 2000. Heat transfer enhancement of nanofluids. *International Journal of Heat and Fluid Flow* 21, 58-64.

Yu, W, Xie, H, Chen, L and Li, L. 2010. Enhancement of thermal conductivity of kerosene-based Fe_3O_4 nanofluids prepared via phase- transfer method. *Colloids and Surfaces A*. 355(1–3), 109–113.

Zhu, H. T. Zhang, C. Y. Tang, Y. M and. Wang, J. X. 2007. Novel synthesis and thermal conductivity of CuO nanofluid, *Journal of Physical Chemistry C*. 111(4) 1646–1650.